Kidney International, Vol. 65 (2004), pp. 871–880

Transdifferentiation of cultured tubular cells induced by hypoxia

KRISSANAPONG MANOTHAM, TETSUHIRO TANAKA, MAKIKO MATSUMOTO, TAKAMOTO OHSE, REIKO INAGI, TOSHIO MIYATA, KIYOSHI KUROKAWA, TOSHIRO FUJITA, JULIE R. INGELFINGER, and MASAOMI NANGAKU

Division of Nephrology and Endocrinology, University of Tokyo School of Medicine, Tokyo, Japan; Molecular and Cellular Nephrology, Institute of Medical Sciences and Department of Medicine, Tokai University School of Medicine, Isehara, Kanagawa, Japan; and Division of Pediatric Nephrology, Massachusetts General Hospital, Boston, Massachusetts

Transdifferentiation of cultured tubular cells induced by hypoxia.

Background. Tubulointerstitial fibrosis leads to progressive kidney disease and, ultimately, may result in end-stage renal disease (ESRD). Myofibroblasts, which express α-smooth muscle actin (α-SMA) in their cytoplasm, regulate renal fibrogenesis. Recent studies suggest that certain interstitial myofibroblasts derive from renal tubular cells that have undergone epithelial-mesenchymal transformation (EMT) (transdifferentiation). However, the role(s) of hypoxia, which is involved in progressive kidney disease, on tubular EMT remains unclear.

Methods Immortalized rat proximal tubular cells (IRPTC) were cultured in normobaric hypoxia (1% O_2) for 3, 6, or 15 days, with match control in normoxic conditions. α-SMA, vimentin, and desmin chosen as markers of EMT were measured by immunocytochemistry and immunoblots collagen I production and cell motility were chosen as functional assays. Various concentrations of cobaltous chloride ($CoCl_2$) were used as hypoxic mimickers. In vivo studies were carried out in a chronic ischemic kidney model.

Results. Immunohistochemical studies revealed increased expression of α-SMA. Striking morphologic changes were detected after 6 days of hypoxia for α-SMA–positive fibroblast-like cells (SMA + fib) and after 15 days for α-SMA–positive myofibroblast-like cells (SMA + myo). Immunoblots confirmed these findings. Collagen I production increased in a time-dependent manner parallel to α-SMA expression. Cell motility assays demonstrated that transformed cells had higher migratory capacity than normal tubular cells. Cobaltous salt also induced α-SMA and collagen I synthesis. Chronic ischemic kidney revealed in vivo tubular EMT at day 7.

Conclusion. Hypoxia can induce tubular EMT. This process may play an important role in progression of kidney disease.

Tubulointerstitial fibrosis is presently considered a final common pathway of progressive kidney disease eventually leading to end-stage renal disease (ESRD) [1–4]. Therefore, understanding the pathogenesis of interstitial fibrosis is crucial for developing therapeutic interventions for kidney diseases. However, the mechanism(s) of renal fibrogenesis are poorly understood.

Tubulointerstitial fibrosis is characterized by the loss of renal tubules and interstitial capillaries and the accumulation of matrix proteins. One of the most remarkable pathologic findings of interstitial fibrosis is the presence of myofibroblasts, which contain alpha-smooth muscle actin (α-SMA) in cytoplasm [5, 6]. In the normal kidney, interstitial myofibroblasts are rare. In contrast, myofibroblasts appear in markedly increased numbers in the fibrotic kidney predominantly within the fibrotic area. Myofibroblasts are morphologically intermediate between fibroblasts and smooth muscle cells. Like fibroblasts, myofibroblasts synthesize collagens I and III [7, 8], while they retain α-SMA expression. Accumulating evidence in both experimental animals and humans has demonstrated correlation both between the presence of myofibroblasts and deterioration of renal function and with long-term prognosis [6, 9–13]. The role of myofibroblasts in the fibrogenic process was also supported by studies showing that once myofibroblasts become detectable in the interstitium, collagen deposition accumulates in the areas in which they reside [14, 15].

The precise origin of myofibroblasts is of interest. Previously, these cells were thought to be derived from circulating bone marrow fibroblasts [16]. However, recent work utilizing chimeric animals showed that renal myofibroblasts were derived de novo from kidney cells [17]. Growing evidence now indicates that myofibroblasts transdifferentiate from tubular cells [i.e., undergoing epithelial to mesenchymal transformation (EMT)]. These then migrate to the interstitium [18]. Apart from tubular cells, a role for EMT is well established in many other types of epithelial cells and is associated with fibrogenesis and neovascularization [19, 20]. The mechanisms of renal tubular EMT are currently the focus of extensive investigations. In vitro data suggest that tubular EMT can

Key words: tubuloitnterstitial fibrosis, transdifferentiation, epithelial mesenchymal transformation, myofibroblast, hypoxia, smooth muscle actin.

Received for publication March 8, 2003
and in revised form July 7, 2003, and September 18, 2003
Accepted for publication October 8, 2003

be induced by profibrotic cytokines such as transforming growth factor (TGF-β1) [21, 22], fibroblast growth factor (FGF) [23], and interleukin-1 (IL-1) [24]. However, a role for hypoxia, which is a critical mediator of kidney disease progression [25], in EMT remains to be elucidated.

According to their higher metabolic demands, proximal tubular cells (PTCs) are more susceptible to hypoxic stimuli [26]. Previous study showed that under hypoxic conditions proximal tubular cells dedifferentiate [27]. The expression of profibrotic factors such as collagen I, TGF-β1, and IL-1 also increases [28]. These changes appear to be mediated via both hypoxia inducible factor (HIF-1α)-dependent and independent pathways [29].

We hypothesized that chronic hypoxia stimulates tubular-myofibroblast transdifferentiation, a crucial step in renal fibrosis. In this present study, we clarified the effect of chronic hypoxia on phenotypic and functional changes of tubular cells in vitro. Our in vivo study supported the role of hypoxia in tubular EMT as well. We also explored hypoxia-induced pathways that are involved in tubular EMT.

METHODS

Cell culture and hypoxic protocol

Immortalized rat proximal tubular cells (IRPTCs) were cultured in Dulbecco's modified Eagle's medium (DMEM) (Nissui Seiyaku, Tokyo, Japan) with 10% $NaHCO_3$, 2 mmol/L HEPES, pH 7.5, and 5% fetal bovine serum (FBS) [30]. For immunohistochemical and motility assays, IRPTC were seeded in 4- or 8-well chamber slides (Lab Trek® II, Nalgen Nunc, Naperville, IL, USA). For immunoblot analyses, IRPTCs were seeded in 6 cm culture dishes. After reaching 50% to 70% confluence, culture dishes were put in a hypoxic (1% O_2, 5% CO_2, 37°C) incubator (Astec Co., Fukuoka, Japan) for 3, 6, or 15 days; control dishes were incubated for equivalent periods under normoxic conditions (21% O_2, 5% CO_2, 37°C). In order to preserve stable hypoxic conditions, the cells in the hypoxic group were periodically examined (every 3 days). The culture media were also changed every 3 days. Changing process was less than 3 minutes for each. In some experiments, cells were passaged if overconfluent. The average time for passaging cells was less than 8 minutes/dish. Each experiment was repeated three to eight times.

Cobaltous chloride ($CoCl_2$)

Since most hypoxic stimuli are mediated via HIF-1α, we used $CoCl_2$ to stabilize HIF-1α without hypoxia. Ten, 30, or 60 μmol/L $CoCl_2$ was added to the culture media for 6-day experiments [31].

Immunohistochemical analyses

At the end of the experiments, cells in 8-chamber slides were fixed with acetone and methanol 1:1 at −20°C for 10 minutes. Direct immunoperoxidase staining was performed as previously described [32]. In brief, endogenous peroxidase was blocked with 3% H_2O_2 for 20 minutes. Nonspecific binding was blocked with 5% nonfat milk in phosphate-buffered saline (PBS) for 5 minutes. Primary antibodies for α-SMA (mouse anti-α-SMA, clone asm-1) (Boehringer Mannheim, Mannheim, Germany), 1:1000, monoclonal mouse antivimentin (V9) (Dako, Glostrup, Denmark), 1:400, monoclonal mouse antidesmin (D33) (Dako) 1:100, or monoclonal mouse anti-HIF-1α, 1:100 (Novus Biological, Littleton, CO, USA), were applied at room temperature for 60 minutes. The slides were incubated with biotinylated antimouse immunoglobulin (Vector Laboratories, Burlingame, CA), 1:400, for 30 minutes, followed by 30 minutes incubation with avidin horseradish peroxidase (Vector Laboratories), 1:2000. Color was developed with 3,3′ diaminobenzidine tetrahydrochloride (DAB), followed by counter-staining with methyl green. For staining HIF-1α, the signal were amplified with tyramide signal amplification (TSA) (Perkin-Elmer, Boston, MA, USA) according to the manufacturer's instruction [33, 34]. The slides were then examined by light microscopy (Olympus BX51, Tokyo, Japan), and pictures were taken by Olympus DP12 system.

Quantitative immunohistochemical analysis

In this study, we observed two phenotypically distinct populations of α-SMA–positive cells. To explore the findings in more detail, we developed a simple classification. The first group was composed of elongated, spindle-shaped hypertrophic cells, as compared to control tubular cells. These cells resemble fibroblasts that contain α-SMA rather than myofibroblasts. We defined these cells as α-SMA positive with fibroblast features (α-SMA + fib). The other group was composed of hypertrophic cells that were strongly positive for α-SMA with many projeted cytoplasmic borders, which is a typical characteristic of myofibroblasts [35]. Thus, we defined this group as α-SMA positive myofibroblasts (α-SMA + myo).

To compare the amount of α-SMA–positive cells in each experiment, cells were systematically counted in nonoverlapping fields, under 400× magnification, from the upper panel to the lower panel of the slide. The numbers of α-SMA + fib, α-SMA + myo, and total α-SMA–positive cells per 1000 cells were measured for each experiment. This process was conducted in a blinded manner twice by the same observer within a 3-week-interval. The mean of these data was used for analysis. The numbers of cells positive for vimentin or desmin were also counted by the same methods per 1000 living cells.

Immunoblots analysis

Tubular cells were plated in 6 cm dishes and were treated with the same protocol as previously described.

At the end of the experiments, culture media were removed, and monolayer cells were washed twice with ice cold PBS, and then were detached with trypsin. Detached cells were collected, spun down at 4°C, 1500 rpm for 5 minutes and washed twice with cold PBS. Cells were then incubated for 30 minutes with ice-cold radioimmunoprecipitation assay (RIPA) buffer [50 mmol/L Tris-Cl, 150 mmol/L NaCl, 1% Nonidet P-40, 0.5% sodium deoyl, 0.1% sodium dodecyl sulfate (SDS)] containing 10 mmol/L phenylmethylsulfonylfluoride (PMSF). Cells were expelled with force through a 23 G needle five times. The homogenized samples were centrifuged at 14,000 rpm for 15 minutes. The supernatants were collected, and protein content was determined with a detergent-compatible Bradford protein assay (BioRad, Hercules, CA, USA) according to the manufacturer's protocol [36]. For measurements of collagen I production, IRPTC and culture media were precipitated in 67% ethanol at 4°C overnight [37]. The precipitated proteins were collected and dissolved in RIPA buffer. The lysates were stored at −20°C until analysis. Equal amounts of protein were mixed with gel loading buffer under reducing conditions (0.25 mol/L Tris-HCl, 4% SDS, 10% sucrose, 0.004% bromphenol blue, 10% 2-mercaptoethanol). Samples were heated at 100°C for 5 minutes and run in 8 or 12% SDS polyacrylamide gels, followed by electrotransfer to polyvinylidine difluoride (PVDF) membrane (Immobilon, Nihon Millipore, Yonezawa, Japan) or Hybond-ECL membrane (Amersham International, Buckingham, UK). The transferred membranes were blocked with 5% nonfat milk in Tris-buffered saline (TBS), 0.01% Tween-20 for 30 minutes at room temperature. The membranes were incubated with polyclonal goat antimouse type I collagen antibody (Southern Biotechnology, Burmingham, AL, USA) at 1:400 for 60 minute at room temperature, or with anti-SMA antibody overnight at 4°C. After extensive wash in TBS, 0.01%Tween, the bound antibodies were detected with alkaline phosphatase-conjugated secondary antibodies. 5-bromo-4-chloro-3-indolyl phosphate/nitro blue tetrazolium tablets (Sigma Fast) (Sigma Chemical Co., St. Louis, MO, USA) were used as a substrate. In some experiments, the bound antibodies were detected by the enhanced chemiluminescence system, ECL (Amersham International).

Apoptosis and cell toxicity assay

Cell toxicity was evaluated by measuring absolute lactate dehydrogenase (LDH) concentrations (Sigma Diagnostics, St. Louis, MO, USA) in culture media at each change (every 3 days) [38]. The floating cells were counted by Trypan blue exclusion methods [37]. Apoptosis on a monolayer in each group was detected by in situ DNA fragmentation TACS blue label kit (Trevigen, Gaithersburg, MD, USA) according to the manufacturer's instruction as previous described [32].

Cell motility assay

IRPTC (2×10^5) from the hypoxic group, the normoxic control group, and the $CoCl_2$-treated group were seeded into 4-chamber slides containing the corresponding culture media. Twenty-four hours after passage, cells formed confluent monolayers. Cuts of 850 ± 43.2 micron width were made with a sterile scalpel. The cells were immediately washed with PBS to remove all the injured cells and cytokines. PBS was then replaced with new equivalent culture media, and the cells were incubated for 4 and 12 hours to allow migration [39]. This whole process was performed in less than 5 minutes. After 4 and 12 hours, cells were fixed with acetone and methanol as described above. These cells were stained with methyl green alone or with anti-αSMA and methyl green counterstaining in other experiments. The width of the scratch was measured with NIH imaging system, by selecting the three narrowest parts, at least 50 microns apart; the means of three narrowest distances were employed to calculate the motility distance for each experimental group.

$$\text{Motility distance} = \frac{850 - \text{scratch width microns}}{2}$$

In vivo study: ischemic nephropathy

Six male Sprague-Dawley rats were subjected to induced ischemic nephropathy as previously described by Troung et al [40]. In brief, rats were general anesthetize with diethyl ether. After identification of the left renal artery, a 26 G needle was placed along the renal artery. Both artery and needle were ligated with silk twice 0.9 cm apart, and then the needle was removed. Twenty-four–hour urines were collected before the operation and at day 7 after the surgery. At day 7, the ischemic kidneys and contralateral kidneys were removed and overnight fixed in Methyl Carnoy's solution, followed by paraffin embedding. The rehydrated tissues were processed to stain periodic acid-Schiff (PAS) and α-SMA as described above.

Statistical analysis

All numerical data were presented in mean ± SD. One-way analysis of variance (ANOVA) with post hoc analysis by least significant different (LSD) method (SPSS for Windows, version 10.0) was employed to determine the difference among the groups. The significant level was set at $P < 0.05$.

RESULTS

Chronic hypoxia-induced phenotypic changes in PTCs with de novo expression of α-SMA

Light microscopic examination showed that IRPTC assumed a cuboidal shape under normoxic conditions. These cells formed a cobblestone-like monolayer typical of tubular cells. Immunohistochemical staining for

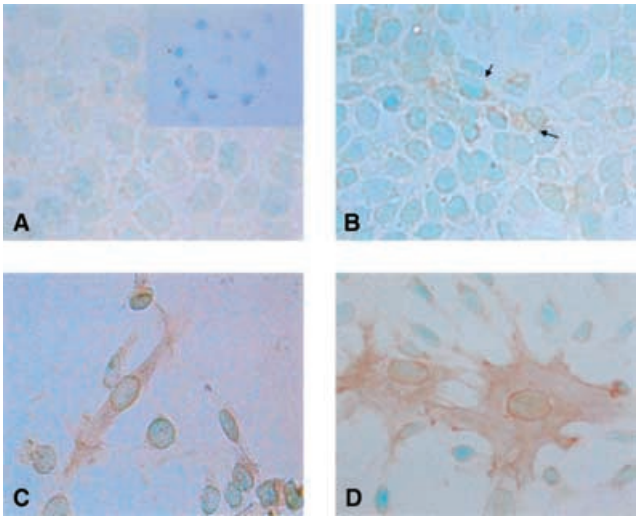

Fig. 1. Immunohistochemical analysis for α-smooth muscle actin (α-SMA) expression. (*A*) Normal immortalized rat proximal tubular cells (IRPTC) were negative for α-SMA staining. Cells were cuboidal in shape and arranged in a cobble stone monolayer. Inset showing IRPTC cultured at a low density. (*B*) After 3 days of hypoxia, some IRPTC expressed α-SMA (arrowhead), but the changes in cell morphology were hardly detectable. (*C*) After 6 days of hypoxia, many IRPTC were elongated in shape with dense α-SMA expression in a filamentous form indicating typical α-SMA + fib morphology (pictures were taken at the border of monolayers in order to show cell morphology). (*D*) Fifteen days of hypoxia induced advanced morphologic changes in some α-SMA–positive IRPTC. These cells were enlarged and had many bifurcates in their cytoplasm with marked expression of α-SMA. These cells were defined as α-SMA + myo (pictures were taken at the border of monolayers in order to show cell morphology).

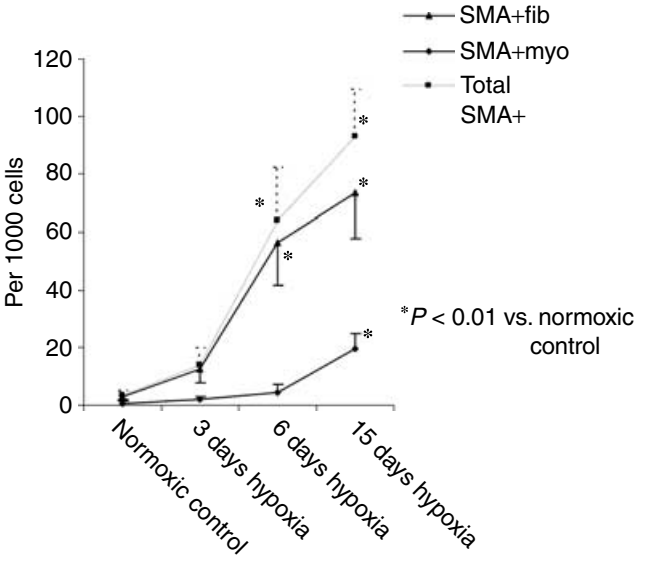

Fig. 2. An increase in the number of α-smooth muscle actin (α-SMA)–positive cells was dependent on hypoxic time.

α-SMA, vimentin, and desmin were all negative under normoxic conditions (Fig. 1A). These characteristics were stable for all cells cultured under normoxic conditions in this study.

After 3 days of hypoxia, some tubular cells expressed α-SMA in their cytoplasm, but morphologic changes were not detected (Fig. 1B). α-SMA staining was more intense after 6 days of hypoxia, and significant morphologic changes were observed at this time point. Most of the α-SMA–positive cells were now elongated in shape and larger than control tubular cells cultured under normoxia, and were designated as α-SMA + fib (Fig. 1C). For the longest period of hypoxia (15 days), phenotypic and morphologic changes were more easily observed (Fig. 1D), with some cells larger than control tubular cells, demonstrating intense and filamentous expression of α-SMA with bifurcations in the cell borders, characteristic of myofibroblasts, and were designated as α-SMA + myo.

An increase in the number of α-SMA–positive cells appeared to be dependent on incubation time under hypoxia

Semiquantitative analysis revealed that expression of α-SMA and phenotypic changes in hypoxia increased in a time-dependent manner (Fig. 2). The number of α-SMA–positive cells was significantly increased after incubation in hypoxia for 6 and 15 days (63.7 ± 18.29 and 92.69 ± 16.17 per 1000 cells, respectively), as compared to 3.33 ± 1.29 per 1000 cells ($P < 0.001$). The number of α-SMA + fib was significantly increased after 6 days of hypoxia (56 ± 14.36) and after 15 days of hypoxia (73.22 ± 15.63) as compared to that of the control group (3.06 ± 0.01) ($P < 0.001$). α-SMA + myo was significantly increased after 15 days of hypoxia.

Hypoxia failed to induce expression of vimentin or desmin in tubular cells

In addition to α-SMA, vimentin and desmin are mesenchymal markers of some subtypes of myofibroblasts (V-type, VD-type myofibroblast) [33]. Hypoxia failed to induce expression of desmin or vimentin in IRPTC (Fig. 3A and B). The amount of desmin or vimentin did not differ between the hypoxic cells and equivalent controls (Fig. 3C), suggesting that hypoxia per se did not induce expression of vimetin or desmin in IRPTC.

Immunoblots analysis confirmed an increase in α-SMA expression

We carried out the immunoblots analysis to confirm our immunohistochemical results. The expression of α-SMA in normoxic control was very little, while α-SMA was increased in a time dependent manner under hypoxic conditions, which was consistent with the immunohistochemical analysis (Fig. 4).

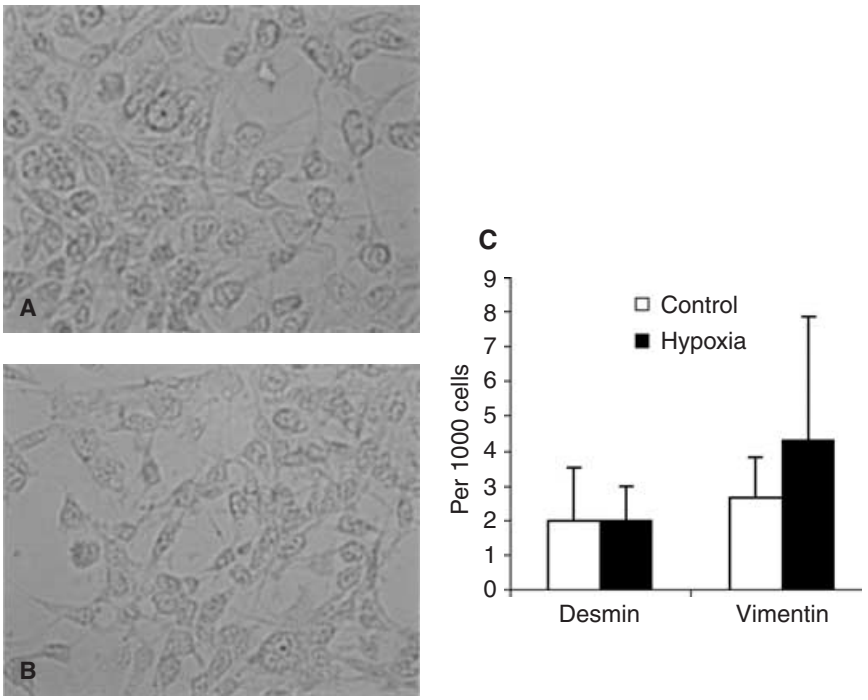

Fig. 3. Hypoxia failed to induce desmin (*A*) and vimentin (*B*) expression (representative pictures were taken from the border zone of 15 days hypoxia experiments). Semiquantitative scoring showed that the numbers of desmin or vimentin positive cells were not increased by hypoxia (*C*) (pool data of 3, 6, and 15 days; $N = 3$ each) (P value = 1 for desmin and 0.4 for vimentin, respectively)

Production of collagen I was increased in hypoxic conditions

Collagen type I is a major component of extracellular matrix in fibrotic kidneys. Immunoblots analysis in the present study demonstrated increased production of collagen type I by IRPTC in hypoxic conditions. Production of collagen type I was observed in a time-dependent manner (Fig. 5).

$CoCl_2$ increased α-SMA expression and collagen I synthesis

Immunohistochemical analysis showed that $CoCl_2$ induced expression of α-SMA in IRPTC in a dose-dependent manner after a 6-day incubation period. Sixty micromol/liter of $CoCl_2$ was most effective in induction of α-SMA expression, whereas lower doses (10 μmol/L) of $CoCl_2$ demonstrated no effect. While $CoCl_2$ induced α-SMA expression, morphologic changes of the treated cells were not as dramatic as those incubated in hypoxia. Most α-SMA–positive cells were smaller than the control cells, and elongated in shape (Fig.6A).

Our immunobloting analysis confirmed these findings. $CoCl_2$ also increased α-SMA expression in a dose-dependent manner (Fig. 6B). Cobalt induced synthesis of collagen type I as well (Fig. 5). These results suggested regulation of these phenotypic changes via the HIF-1α–dependent pathway.

HIF-1α was increased by hypoxia or $CoCl_2$

To confirm the role of hypoxia and a chemical mimicker, we identified HIF-1α by immunocytochemical

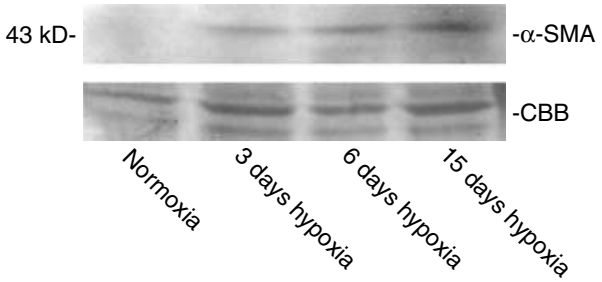

Fig. 4. Immunoblots analysis (top) confirmed increased expression levels of α-smooth muscle actin (α-SMA) in a time-dependent manner. Amount of protein from representative blot (bottom) visualized with Coomassie Brilliant Blue (CBB).

methods. In normoxic conditions, HIF-1 α could not be detected. In contrast HIF-1α was markedly up-regulated in the hypoxic group predominately in the cell nucleus. Cells treated with $CoCl_2$ also showed an increase in expression of HIF-1α (Fig. 7).

Hypoxia increased cell migration of IRPTC

Migration is not a prominent feature of epithelial cells, including tubular cells. In contrast, interstitial mesenchymal cells, especially myofibroblasts, are motile under physiologic conditions. We tested the motility function to examine functional changes of IRPTC under hypoxic conditions. Four hours after placing a scratch on a monolayer, cells under hypoxic conditions migrated further as compared to normoxic controls. The means of migratory distances were 207.48 ± 92.15, 319.68 ± 52.32, and 386.38 ± 25.95 microns for normoxic, 6 days of hypoxia, and 15 days of hypoxia, respectively. The majority of

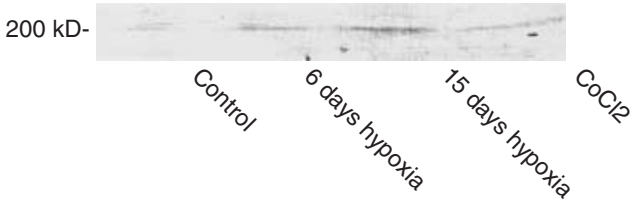

Fig. 5. Immunublot analysis collagen type I production of collagen type I was increased by hypoxia in a time-dependent manner.

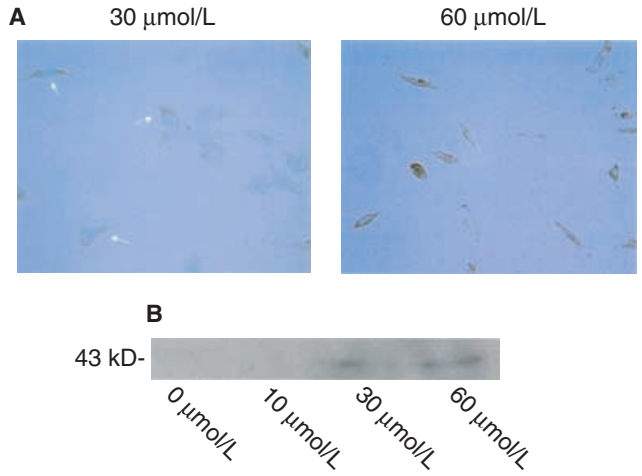

Fig. 6. Cobaltous salt induced α-smooth muscle actin (α-SMA) expression. (*A*) Immunohistochemical study revealed that 6 days of cobaltous chloride ($CoCl_2$) (30 and 60 µmol/L)–treated tubular cells expressed α-SMA. Arrow indicted the α-SMA–positive cells. (*B*) Imunoblotting analysis confirmed the increased amount of α-SMA in immortalized rat proximal tubular cells (IRPTCs) treated with $CoCl_2$.

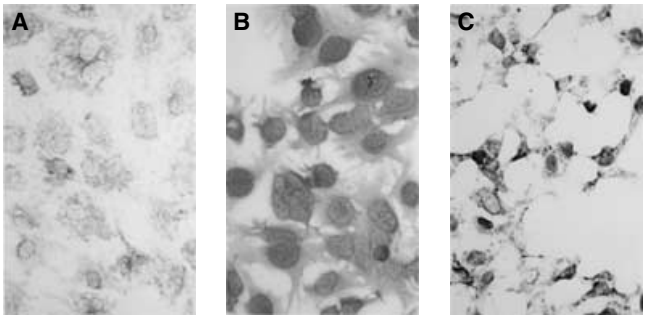

Fig. 7. Immunocytochemical analysis of hypoxia inducible factor-1α (HIF-1*α*). (*A*) Normoxic control did not express HIF-1α in nucleus or cytoplasm. (*B*) Hypoxic immortalized rat proximal tubular cells (IRPTCs) strongly expressed HIF-1α in a nucleus-pattern. (*C*) Six days of cobaltous chloride ($CoCl_2$) treatment of IRPTC also induced HIF-1α expression in their nucleuses.

the mobile cells that migrated to the edge of the migration contained α-SMA in their cytoplasm (Fig. 8). For 12 hours study, the distance between the scratched cells was even less but significant in the normoxic group, while the scratches were completely covered with migrating cells and disappeared in both hypoxic groups (data not shown).

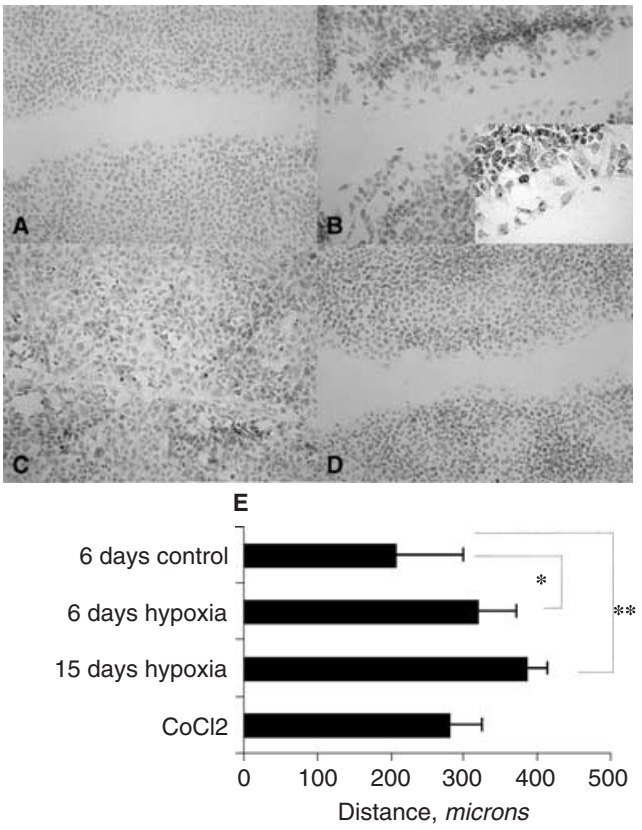

* $P < 0.05$
** $P < 0.01$

Fig. 8. Motility assays. Pictures were taken at 4 hours after a scratch on confluent monolayer were made. (*A*) Normoxic control. (*B*) Six days of hypoxia. Motility distance was increased. Inset shows most of the cells moved to the farthest contained α-smooth muscle actin (α-SMA) in the cytoplasm. (*C*) Fifteen days of hypoxia demonstrated that the scratch was almost covered by migrating α-SMA positive tubular cells (PTCs). (*D*) Treatment with 60 µmol/L cobaltous chloride ($CoCl_2$) did not enhance migration of tubular cells. (*E*) Graph comparing motility distance between each group. Both hypoxic groups showed significantly increased motility capacity.

Hypoxia of our condition did not increase apoptosis or significant cell cytotoxicity

Supernatant LDH concentrations and Trypan blue exclusion assays in each media change did not differ between hypoxic and match normorxic control (data not shown). The excretory amount of LDH per total LDH in the normoxic control was 21.41% ± 0.79% while that of hypoxic were 22.36% ± 1.97%, 21.16% ± 0.82%, and 23.17% ± 1.65% for 3,6, and 15 day hypoxia, respectively (Fig. 9G). However, the excretory amount of LDH was increase to 25.42% + 0.71% in 6 days of 60 µmol/L cobalt group. In situ DNA fragment labeling assay showed that apoptosis did not increase. The number of apoptosis cells in control was 35.5 ± 6.1 per thousand cells. In hypoxic groups, the number of apoptosis cells was 23.4 ± 2 per thousand cells for 3-day hypoxia and 43.3 ± 5.6, 41.1 ± 5.5 per thousand cells for 6- and 15-day hypoxia, respectively

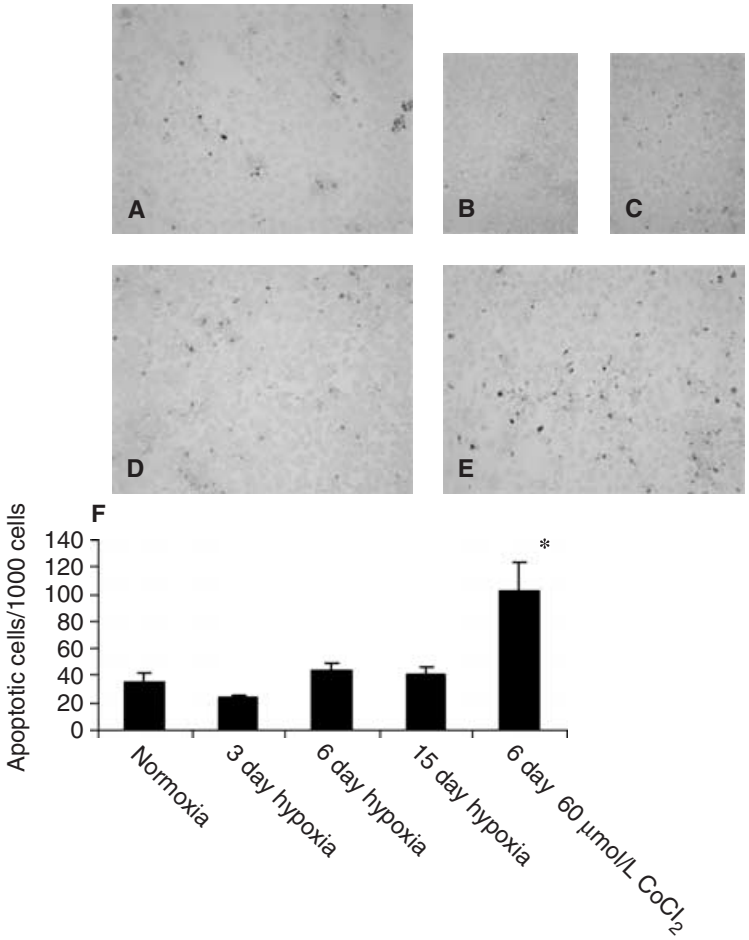

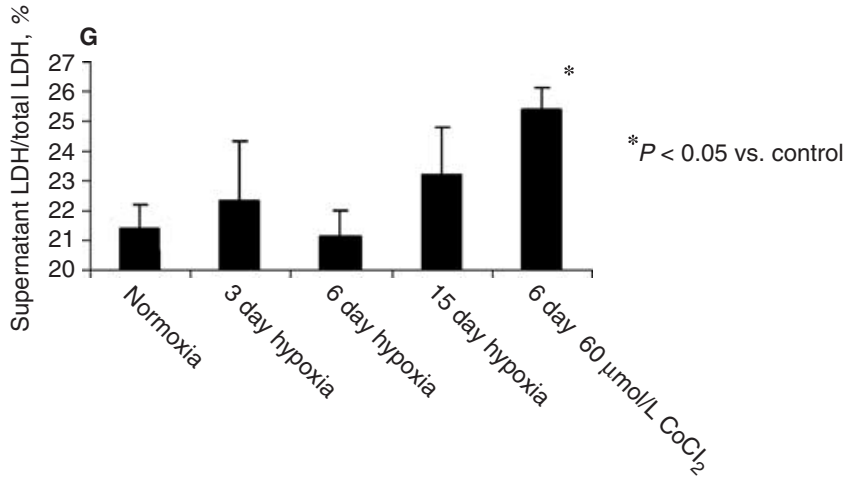

Fig. 9. In situ DNA fragmentation labeling of immortalized rat proximal tubular cells (IRPTC). Confluent normoxic control (picture was taken from 3-day control). (*A*) Three, 6, and 15 days of hypoxia showing the number of apoptosis cells did not significantly increase (*B* to *D*). However, 6 days of cobaltous chloride ($CoCl_2$) 60 µmol/L slightly increased apoptosis (*E*). Graph comparing the number of apoptosis cells in each experiment only 6-day of 60 µmol/L $CoCl_2$ significantly increase apoptosis; however, the majority of cells remained survive (*F*). Graph showing the amount of culture media lactate dehydrogenase (LDH)/total LDH in each group (*G*). Amount of LDH did not differ between normoxic control and hypoxia; only with high-dose cobalt that LDH increases. Wide error bars in the hypoxic groups might indicate some toxic effects of hypoxia.

(Fig. 9A–D, F). Cobalt increased cell apoptosis. The number of apoptosis cells in 6 day of 60 µmol/L cobalt increase to 102.2 ± 20.8 per thousand cells ($P < 0.05$ ANOVA). At any rate, the majority of cells remained survived (Fig. 9E and F). This data suggested the toxicity of chemical hypoxic mimicker and might explain the discrepancy of our finding between cobalt and hypoxic stimuli.

In vivo transdifferentiation of tubular cells was induced by chronic ischemia of the kidney

To support the role of hypoxia in transdifferrentiation, we induced chronic ischemic nephropathy in rats. Our data showed that severe tubulointerstitial damage rapidly developed as early as 1 week after induce ischemia (Fig. 10). At this time point, the amount of urinary protein

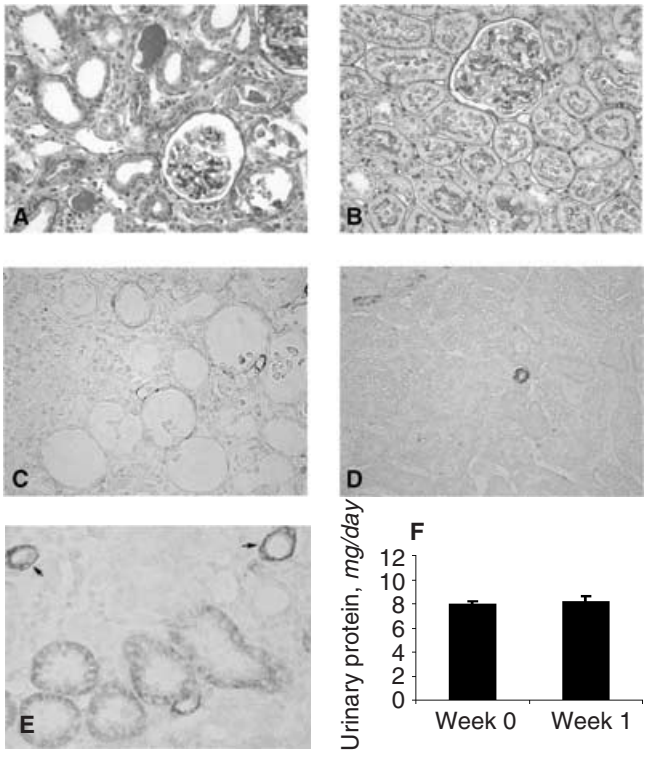

Fig. 10. In vivo studies of a chronic ischemic nephropathy model. After 7 days, the chronic ischemic kidneys developed severe tubulointerstitial damage and fibrosis, whereas the contralateral kidneys remained normal, as shown by periodic acid-Schiff (PAS) staining of chronic ischemic kidneys (*A*) and contralateral controls (*B*). Immunohistochemical analysis for α-smooth muscle actin (α-SMA) showed many α-SMA–positive interstitial cells, while tubular cells and interstitial cells in contralateral kidneys did not express α-SMA (*C*). (*D*) High magnification view showed that some tubules in chronic ischemic kidneys strongly expressed α-SMA (compare to the neighboring arteriole indicated by an arrow) (*E*). (*F*) Graph showing the amount of 24-hour urine protein excretion did not increase.

excretion did not increase. Immunohistochemical studies of α-SMA demonstrated a markedly increase of myofibroblasts in the interstitial area. Some tubular cells strongly expressed SMA, indicating in vivo transdifferentiation. In contrast, the contralateral kidneys remained normal.

DISCUSSION

Accumulating evidence suggests that chronic hypoxia is involved in progressive kidney disease. Recent works have emphasized that the loss of peritubular capillary begins during the early period of renal disease, preceding the development of tubulointerstitial fibrosis and aggravating tubulointerstitial hypoxia. We previously showed that peritubular capillary loss occurred in a thrombotic microangiopathy model [41, 42] while others reported similar findings in remnant kidneys [43], unilateral ureteral obstruction (UUO) [44], and an anti-glomerular basement membrane (GBM) nephritis model [45]. In the present study, we demonstrated the transdifferentiation of tubular cells by hypoxia, as indicated by de novo expression of a mesenchymal marker, morphologic changes, and acquisition of mobility. Furthermore, we demonstrated in vivo EMT in a chronic ischemic model of the kidney. Taken together, our results supported the role of hypoxia in EMT, which is a crucial process in renal fibrogenesis [46]. We also propose that the mechanism of hypoxia-induced EMT may be, at least in part, regulated by the HIF-1α–dependent pathway.

Hypoxia has many effects on higher eukaryotic cells. Transcription of many genes is regulated by hypoxic stimuli via hypoxia-inducible factors, including vascular endothelial growth factor (VEGF), erythropoietin (EPO), glucose transporter (GLUT) and heme oxygenase-1 (HO-1) [47]. A variety of profibrotic cytokines are also up-regulated by hypoxia [37, 48, 49]. For long-term adaptation to hypoxia, cells reduce protein synthesis, turn off unnecessary membrane channels, and decrease cellular activities [27, 50]. Our work suggests unusual responses of tubular cells by changing their phenotypes. The number of α-SMA–positive cells began to increase after 3 days and reached a plateau in two weeks of hypoxia. The immunoblots data also supported these results. Morphologic changes appeared somewhat later. After 6 days of hypoxia, we observed characteristic myofibroblast-like morphology in α-SMA–positive cells. It is likely that expression of α-SMA and EMT may involve many genes and various steps of cell adaptation. The time course of EMT in our study is consistent with previous reports [21]. Yang and Liu [51] and Yang et al [52] previously showed that EMT needs many steps before completion of transdifferentiation. However, in this present study, hypoxia per se could not induce the expression of vimentin and desmin in our tubular cell line. These two antigens are expressed in some, but not all, myofibroblasts. Studies in liver and lung fibrosis showed that α-SMA–positive vimentin-negative myofibroblasts participate in the pathogenesis of this process [8, 53].

In addition to expression of new mesenchymal antigens, loss of normal cytoskeletal and cell-to-cell adhesion molecules is considered as a part of the EMT process [18, 21–23]. In the present study, we avoided testing the loss of these antigens because loss of normal structures by noxious stimuli such as hypoxia does not provide conclusive evidence of transformation. In contrast, hypoxic tubular cells gained motility function, generally not a feature of epithelial cells. Increased cell motility has been reported as one of the features of EMT [54, 55]. Since motility is an active and energy-consuming process, it is surprising that hypoxic cells treated for the longest period, which should lead to the most severe energy depletion, showed the highest motility. Furthermore, in our motility study, we found that most of the leading edge cells contained α-SMA in their cytoplasm. We also measured the amount

Table 1. Summary of epithelial-mesenchymal transformation (EMT) data

	Control	Hypoxia			$CoCl_2$
		3 days	6 days	15 days	
Morphology of cell	Cuboidal	Cuboidal	Elongated	Elongated, bifurcated	Elongated
Size of transformed cell	NC	NC	Larger	Larger	Smaller
α-SMA	–	+	+++	++++	+++
Desmin	–	–	–	–	–
Vimentin	–	–	–	–	–
Collagen I	+	NA	++++	++++	++++
Migration	+	NA	++++	+++++	+

Abbreviations are: $CoCl_2$, coblaltous chloride; α-SMA, α-smooth muscle actin; NA, not available; NC, no change.

of collagen I, a major component of the extracellular matrix, which accumulates in fibrotic tissues. Opharnides, Fine, and Norman [28] demonstrated increased collagen I synthesis by PTCs in hypoxic conditions. We confirmed and extended their findings, clarifying that amount of collagen I increased in a time-dependent manner and was strongly paralleled to EMT. We speculate that the transformed cells may take part in fibrogenesis via collagen I synthesis.

Cobaltous salt is well established as a chemical mimicker of hypoxia by stabilizing HIF1α [33, 37, 47]. In our study, α-SMA expression and collagen synthesis were induced by $CoCl_2$ in a dose-dependent manner. Immunohistochemical analysis of HIF-1α confirmed upregulation of HIF-1α in both hypoxic- and cobalt-treated groups. These results suggest that HIF-1α may also be involved in tubular EMT-induced by hypoxia. However, LDH assay and apoptosis study suggested that cobalt had additional cytotoxicity compared to hypoxia; therefore, not all aspects of EMT could be induced by cobalt (Table 1)

In addition to the results of these in vitro studies, phenotypic changes of renal tubular cells were observed in many experimental models as well as in human diseases [18, 56–58]. It is possible that disruption of the tubular basement membrane, proteinuria, or infiltrative macrophages may play a role in in vivo transdifferentiation of tubular cells, the loss of peritubular capillaries and subsequent hypoxia in tubulointerstitial compartment in remnant kidneys may also be important [59]. Our in vivo experiments in chronic ischemic kidneys provided suggestive evidences that chronic ischemia/hypoxia might induce tubulointersitial fibrosis, as previously described [40] and tubular EMT. Since we did not observe significant proteinuria, this result strongly supported a role of hypoxia in EMT and progression of renal fibrosis.

CONCLUSION

Our work demonstrates an important role of hypoxia in tubular EMT, a crucial step in renal fibrosis and progression of kidney disease. This insight may lead to novel therapeutic interventions of chronic renal disease in the future.

ACKNOWLEDGMENTS

This work was supported by Scientific Grant by Novartis. We thank Dr. Ryoji Sassa (Okazaki Kita Clinic, Nagoya, Japan) and Dr. Kriang Tungsanga (Division of Nephrology, Chulalongkorn University Hospital, Bangkok, Thailand) for their generous support.

Reprint requests to Masaomi Nangaku. University of Tokyo School of Medicine, Division of Nephrology and Endocrinology, 7-3-1 Hongo Bunkyo-Ku, Tokyo, Japan.
E-mail: mnangaku-tky@umin.ac.jp

REFERENCES

1. Nath KA: Tubulointerstitial changes as a major determinant in progression of renal damage. *Am J Kidney Dis* 1:1–17, 1992
2. Eddy AA: Molecular insights into renal interstitial fibrosis. *J Am Soc Nephrol* 7:2495–508, 1996
3. Remuzzi G, Bertani T: Pathophysiology of progressive nephropathies. *N Engl J Med* 339:1448–1456, 1998
4. Klahr S: Progression of chronic renal disease. *Heart Dis* 3:205–209, 2001
5. MacPherson BR, Leslie KO, Lizaro KV, Schwarz JE: Contractile cells of the kidney in primary glomerular disorders: An immunohistochemical study using anti-alpha-smooth muscle actin monoclonal antibody. *Hum Pathol* 24:710–6, 1993
6. Alpers CE, Hudkins KL, Floege J, Johnson RJ: Human renal cortical interstitial cells with some features of smooth muscle cell participate in tubulointerstitial and crecentic glomerular injury. *J Am Soc Nephrol* 5:201–209, 1994
7. Tang WW, Van Gy, Qi M: Myofibroblast and alpha 1(III) collagen expression in experimental tubulointerstitial nephritis. *Kidney Int* 51:926–931, 1997
8. Hogemann B, Gillessen A, Bocker W, *et al*: Myofibroblast-like cells produce mRNA for type I and III procollagens in chronic active hepatitis. *Scand J Gastroenterol* 28: 591–594, 1993
9. Diamond JR, van Goor H, Ding G, Engelmyer E: Myofibroblasts in experimental hydronephrosis. *Am J Pathol* 146:121–129, 1995
10. Hewitson TD, Wu HL, Becker GJ: Interstitial myofibroblasts in experimental renal infection and scarring. *Am J Nephrol* 15:411–417, 1995
11. Hewitson TD, Becker GJ: Interstitial myofibroblasts in IgA glomerulonephritis. *Am J Nephrol* 15:111–117, 1995
12. Roberts IS, Burrows C, Shanks JH, *et al*: Interstitial myofibroblasts: Predictors of progression in membranous nephropathy. *J Clin Pathol* 50:123–127, 1997
13. Essawy M, Soylemezoglu O, Muchaneta-Kubara EC, *et al*: Myofibroblasts and the progression of diabetic nephropathy. *Nephrol Dial Transplant* 12:43–50, 1997
14. Badid C, Vincent M, McGregor B, *et al*: Mycophenolate mofetil reduces myofibroblast infiltration and collagen III deposition in rat remnant kidney. *Kidney Int* 58:51–61, 2000
15. Pichler RH, Hugo C, Shankland SJ, *et al*: SPARC is expressed in renal interstitial fibrosis and in renal vascular injury. *Kidney Int* 50:1978–1989, 1996
16. Bucala R, Spiegel LA, Chesney J, *et al*: Circulating fibrocytes define a new leukocyte subpopulation that mediates tissue repair. *Mol Med* 1:71–81, 1994
17. Iwano M, Plieth D, Danoff TM, *et al*: Evidence that fibroblast derive from epithelium during tissue fibrosis. *J CIin Invest* 110:341–350, 2001
18. Ng YY, Huang TP, Yang WC, *et al*: Tubular epithelial-myofibroblast transdifferentiation in progressive tubulointerstitial fibrosis in 5/6 nephrectomized rats. *Kidney Int* 54:864–876, 1998
19. Piek E, Moustakas A, Kurisaki A, *et al*: TGF-β type1 receptor/ALK-5 and Smad proteins mediated epithelial to mesenchymal transdifferentiation in NMuMG breast epithelial cells. *J Cell Sci* 112:4557–4588, 1999

20. Rockey DC: The cell and molecular biology of hepatic fibrogenesis. Clinical and therapeutic implications. *Clin Liver Dis* 4:329–355, 2000
21. Fan JM, Ng YY, Hill PA, *et al*: Transforming growth factor β regulates tubular epithelial-myofibroblast transdifferentiation in vitro. *Kidney Int* 56:1455–1467, 1999
22. Li JH, Zhu HJ, Huang XR, *et al*: Smad7 inhibits fibrotic effect of TGF-β on renal tubular epithelial cell by blocking Smad2 activation. *J Am Soc Nephrol* 13:1464–72, 2002
23. Strutz F, Zeisberg M, Ziyadeh FN, *et al*: Role of basic fibroblast growth factor-2 in epithelial-mesenchymal transformation. *Kidney Int* 61:1714–1728, 2002
24. Vesey DA, Cheung CW, Cuttle L, *et al*: Interleukin 1-β induce human proximal tubule injury, α-smooth muscle actin expressin and fibronectin production. *Kidney Int* 62:31–40, 2002
25. Fine LG, Bandyopadhay D, Norman JT: Is there a common mechanism for the progression of different types of renal disease other than proteinuria? Towards the unifying theme of chronic hypoxia. *Kidney Int* 57(Suppl 75) S22–S26, 2000
26. Lieberthal W, Nigam SK: Acute renal failure. I. Relative importance of proximal vs. distal tubular injury. *Am J Physiol* 275:F623–F632, 1998
27. Sahai A, Mei C, Zavosh A, Tannel RL: Chronic hypoxia induces LLC-PK_1 cell proliferation and dedifferentiation by the activation of protein kinase C. *Am J Physiol* 272:F809–F815, 1997
28. Orphanides C, Fine LG, Norman JT: Hypoxia stimulates proximal tubular cell matrix production via TGF-β1 independent mechanism. *Kidney Int* 52:637–647, 1997
29. Norman JT, Clark IM, Garcia P: Regulation of TIMP-1 expression by hypoxia in kidney fibroblast. *Ann NY Acad Sci* 878:503–505, 1999
30. Tang SS, Jung F, Diamant D, *et al*: Temperature sensitive SV40 immortalized rat proximal tubule cell line has functional renin-angiotensin system. *Am J Physiol* 268:F435–F446, 1995
31. Gong P, Hu B, Stewart D, *et al*: Cobalt induces heme oxygenase-1 expression by hypoxia-inducible factor-independent mechanism in Chinese hamster ovary cells regulation by Nrf2 and MafG transcription factors. *J Biol Chem* 276:27018–27025, 2001
32. Shao J, Miyata T, Yamada K, *et al*: Protective role of nitric oxide in a model of thrombotic microangiopathy in rats. *J Am Soc Nephrol* 12:2088–2097, 2001
33. Matsumoto M, Makino Y, Tanaka T, *et al*: Induction of renoprotective gene expression by cobalt ameliorate ischemic injury of the kidney in rats. *J Am Soc Nephrol* 14:1825–1832, 2003
34. Rosenberger C, Mandriotas S, Jurgensen JS, *et al*: Expression of hypoxia-inducible factor-1alpha and -2alpha in hypoxic and ischemic rat kidneys. *J Am Soc Nephrol* 13:1721–1732, 2002
35. Powell DW, Mifflin RC, Valentich JD: Myofibroblasts. I. Paracrine cells important in health and disease. *Am J Physiol* 277: C1–C19, 1999
36. Bradford MM: A rapid and sensitive method for the quantitation of microgram quantities of protein utilizing the principle of protein-dye binding. *Anal Biochem* 72:248–254, 1976
37. Norman JT, Clark IM, Garcia P: Hypoxia promotes fibrogenesis in human renal fibroblast. *Kidney Int* 58:2351–2366, 2000
38. Nangaku M, Quigg RJ, Shankland SJ, *et al*: Over expression of Crry protects mesangial cells from complement-mediated injury. *J Am Soc Nephrol* 8:223–233, 1997
39. Prest SJ, May FE, Westley BR: The estrogen-regulated protein TFF-1, stimulates migration of human breast cancer cells. *FASEB* 16:592–594, 2002
40. Truong LD, Farhood A, Tasby J, Gillum D: Experimental chronic renal ischemia: Morphological and immunohistochemical studies. *Kidney Int* 41:1676–1689, 1992
41. Nangaku M, Alpers CE, Pippin J, *et al*: A new model of renal microvascular endothelial injury. *Kidney Int* 52:182–194, 1997
42. Nangaku M, Yamada K, Gariepy CE, *et al*: ET_B receptor protects the tubulointerstitium in experimental thrombotic microangiopathy. *Kidney Int* 62:922–928, 2002
43. Kang DH, Joly AH, Oh SW, *et al*: Impaired angiogenesis in the remnant kidney model. I. Potential role of vascular endothelial growth factor and thrombospondin-1. *J Am Soc Nephrol* 12:1434–1447, 2001
44. Ohashi R, Shimizu A, Masuda Y, *et al*: Peritubular capillary regression during the progression of experimental obstructive nephropathy. *J Am Soc Nephrol* 13:1795–805, 2002
45. Ohashi R, Kitamura H, Yamanaka N: Peritubular capillary injury during the progression of experimental glomerulonephritis in rats. *J Am Soc Nephrol* 11:47–56, 2000
46. Stutz F, Muller GA: Transdifferentiation comes of age. *Nephrol Dial Transplant* 15:1729–1731, 2000
47. Wenger RH: Cellular adaptation to hypoxia: O_2-sensing protein, hydroxylase, hypoxia-inducible transcription factors and O_2-regulated gene expression. *FASEB J* 16:1151–1162, 2002
48. Saed GM, Zhang W, Dimond MP: Effect of hypoxia on stimulation effect of TGF-β1 on MMP-2 and MMP-9 activities in mouse fibroblast. *J Soc Gynecol Invest* 7:348–354, 2000
49. Falanga V, Zhou L,Yufit T: Low oxygen tension stimulates collagen synthesis and COL1A1 transcription though the action of TGF-β1. *J Cell Physiol* 191:42–50, 2002
50. Hochachka PW, Lutz PL: Mechanism, origin, and evolution of hypoxia tolerance. *Comp Biochem Physiol B Biochem Mol Biol* 130:435–459, 2001
51. Yang J, Liu Y: Dissection of key events in tubular epithelial to myofibroblast transition and its implications in renal interstitial fibrosis. *Am J Pathol* 159:1465–1475, 2001
52. Yang J, Shultz RW, Mars WM, *et al*: Disruption of tissue-type plasminogen activator gene in mice reduces renal interstitial fibrosis in obstructive nephropathy. *J Clin Invest* 110:1525–1538, 2002
53. Zhang K, Rekhter MD,Gordon D, Phan SH: Myofibroblasts and their role in lung collagen gene expression during pulmonary fibrosis. *Am J Pathol* 145:114–125, 1994
54. Hay ED, Zuk A: Transformations between epithelium and mesenchyme: Normal, pathological, and experimentally induced. *Am J Kidney Dis* 26:678–690, 1995
55. Zuk A, Matlin KS, Hay ED: Type I collagen gel induces Madin-Darby canine kidney cells to become fusiform in shape and lose apical-basal polarity. *J Cell Biol* 108:903–919, 1989
56. Okada H, Inoue T, Kanno Y, *et al*: Renal fibroblast-like cells in Goodpasture's syndrome rats. *Kidney Int* 60:597–606, 2001
57. Okada H, Ban S, Nagao S, *et al*: Progressive renal fibrosis in murine polycystic kidney disease: An immunohistochemical observation. *Kidney Int* 58: 587–597, 2000
58. Abbate M, Zoja C, Rottoli D, *et al*: Proximal tubular cells promote fibrogenesis by TGF-beta1-mediated induction of peritubular myofibroblasts. *Kidney Int* 61:2066–2077, 2002
59. Kang DH, Kanellis J, Hugo C, *et al*: Role of the microvascular endothelium in progressive renal disease. *J Am Soc Nephrol* 13:806–816, 2002